

Brevia

A simple graphical method for estimating the components of the fault-slip vector

CARLOS H. COSTA, JUAN C. CESCO* and RICARDO J. MORÁN

Universidad Nacional de San Luis, Chacabuco 917, 5700 San Luis, Argentina

(Received 2 July 1996; accepted in revised form 19 May 1997)

Abstract—A simple calculation of the components of the total slip vector (D) on a fault plane allows the relationships between the magnitudes of the three slip components of D , the lateral horizontal displacement (L), the transversal horizontal displacement (T) and the vertical offset (V), to be determined. The contribution of each slip component to the total slip can be plotted jointly in a ternary diagram, assuming a unit length of the vector modulus and a suitable normalization for D . Each component equals the magnitude of D at the vertices of the diagram, hence it is possible to estimate the percentage contribution of each slip component to the total movement of a fault or a set of faults. The dip of the fault surface and the rake of the slickenlines are the input data required for displaying L , T and V relationships in these diagrams. This information may be useful in the analysis of movement geometry for different fault populations and in the determination of D by measuring just one of the fault-slip components, such as vertical slip associated with a fault scarp. © 1997 Elsevier Science Ltd.

PRINCIPLES

Evaluation of the geometrical characteristics of fault slip is an important first step in the tectonic analysis of fault-slip data. This is generally done prior to the kinematic-dynamic analysis or palaeostress reconstruction. The geometric analysis of fault slip can be carried out even if data reliability is less than that normally required for the kinematic-dynamic analysis, as only dip and rake (pitch) angles are necessary.

The basic principle of the graphical representation proposed here assumes that slip on a fault surface takes place along the projection of the maximum shear stress direction in that plane. This projection is represented by the slickenlines (Bott, 1959; Angelier, 1979, 1984, 1994). Accordingly, the total slip vector (D) has the same orientation as the slickenlines.

The magnitude of D generally remains unknown but, by assuming a unit length, it is possible to calculate the relative values of the three slip components of the total fault movement. This calculation can be achieved by means of simple trigonometric relationships. The total displacement vector (D) of a fault can be decomposed into three components: lateral horizontal displacement (L), transversal horizontal displacement (T) and vertical displacement (V) (Angelier, 1979, 1994). The necessary input data for the resolution of these components are the dip angle (β) of the fault plane and the rake angle of the slickenside lination (δ) in the plane of the fault. With D assigned a unitary value, then L , V and T can be expressed by the following relations (Fig. 1):

$$L = \cos \delta \tag{1}$$

$$T = \sin \delta \cdot \cos \beta \tag{2}$$

$$V = \sin \delta \cdot \sin \beta \tag{3}$$

where $D^2 = L^2 + T^2 + V^2$.

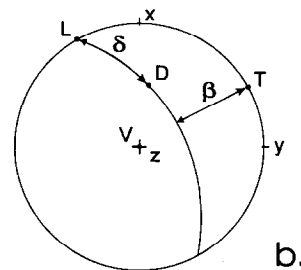
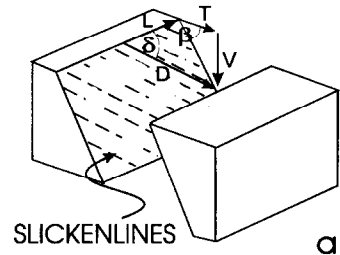


Fig. 1. (a) Angular relationships of the three slip components: horizontal longitudinal slip (L), horizontal transversal slip (T) and vertical slip (V). β , dip of the fault plane; δ , rake of the slickenlines. (b) Stereographic representation in an equal-angle net (lower-hemisphere) of the geometrical relationships displayed in (a). +x, north; +y, east; +z, down.

*Also at: Centro Regional de Estudios Avanzados-IMASL-CONICET, Puente Blanco, 5700 San Luis, Argentina.

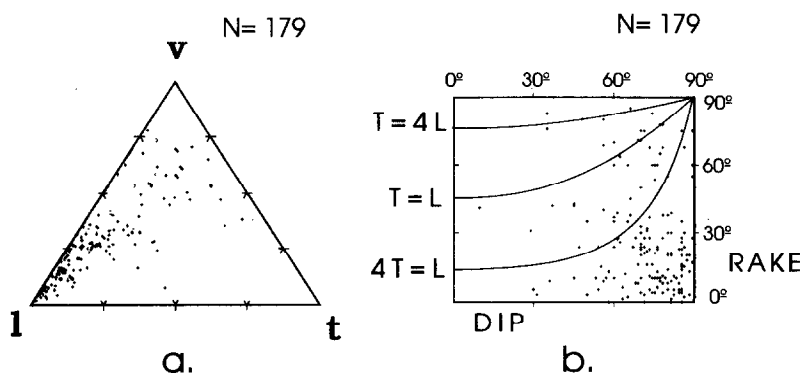


Fig. 2. Data representation in a fault-slip component diagram (FSC). (a) showing the predominance of strike-slip movements. Component l , and consequently the horizontal longitudinal slip (L), is over 75% of the total slip for the majority of the fault population. (b) The same data plotted in terms of dip and rake values.

Angelier (1979) has developed diagrams for estimating relative proportions between two components of D from dip and rake data. A more complete picture of the movement geometry on a fault or a group of faults can be obtained by plotting the relative magnitudes of two slip components as Cartesian coordinates (Angelier, 1984). These relationships are expressed as a ratio of D , instead of dip and rake angles. Angelier also suggested that the L vs T relationship, for instance, is more relevant regarding the general deformation of a rock mass than dip and rake angles. A comparative analysis on the proportional contribution of each slip component to the total displacement of a fault requires three separate plots (L vs T , L vs V and T vs V).

However, a different approach is adopted here considering that vector D is, in fact, a direction. Because it has been assigned a unit length, its direction is equivalently represented by a point on a sphere of unit radius. Hence, it is more convenient to choose another normalization (v for V), namely the norm 1 normalization. This is the same as representing the direction associated with D by a point on the set of all points satisfying that the sum of the absolute value of their components adds up to 1, and this permits the adoption of a single ternary graph (Fig. 2a). The norm 1 for a vector $v = (v_1, v_2, v_3)$ is given by:

$$v = |v_1| + |v_2| + |v_3|.$$

Therefore, if L , T and V are given by eqns (1)–(3) then d is defined by:

$$d = l + t + v,$$

where l , t and v have the following components:

$$l = \frac{(\cos \delta)}{(|\cos \delta| + |\sin \delta \cdot \cos \beta| + |\sin \delta \cdot \sin \beta|)}$$

$$t = \frac{(\sin \delta \cdot \cos \beta)}{(|\cos \delta| + |\sin \delta \cdot \cos \beta| + |\sin \delta \cdot \sin \beta|)}$$

$$v = \frac{(\sin \delta \cdot \sin \beta)}{(|\cos \delta| + |\sin \delta \cdot \cos \beta| + |\sin \delta \cdot \sin \beta|)}$$

and where $l + t + v = 1$.

The absolute value of each component of the total displacement vector d can be used as an index to measure the degree to which the corresponding slip component contributes to the total slip, and it can be represented graphically by a point on a triangle (Fig. 2). Its position on this diagram is a function of the relative contribution of each slip component to the total slip as described above. For instance, a d vector represented by the vertex t indicates that fault movement was exclusively horizontal transversal slip (T).

EXAMPLES AND APPLICATIONS

The diagram in Fig. 2(a) displays a fault population with a strong cluster near vertex l , indicating that the displacement field is predominantly strike-slip. An important number of faults indicate that l constitutes approximately 0.85 or 85% of the total slip in the fault set. Thus, $l \gg t + v$ and $L \gg T + V$. Consequently, these observations indicate a minimum participation of T in the overall slip, even with respect to V . Such a conclusion is also clear in the two-dimensional diagram of Angelier (1979) (Fig. 2b). L/T ratios for each dip and rake pair on a striated fault surface are indicated here by curves derived from the angular relationships shown in Fig. 1.

Figure 3(a) shows how different trends of slip geometry among fault populations from different data collection localities (fault stations) are distinguished. Data discrimination concerning the sense of movement of each fault-slip plane can also be represented (Fig. 3b), with the aim of providing a more complete insight into the fault-slip geometry. The diagrams developed by Angelier (1979, 1984), as well those proposed here, allow the resolution of the horizontal transversal slip (T) in the overall deformation of a rock body. Such a slip component is commonly underestimated in the fracture analysis, even if it provides a more direct estimate of the shortening/extension rate associated with the faulting.

The total slip (D) can be roughly estimated for a given fault population if the magnitude of a single component

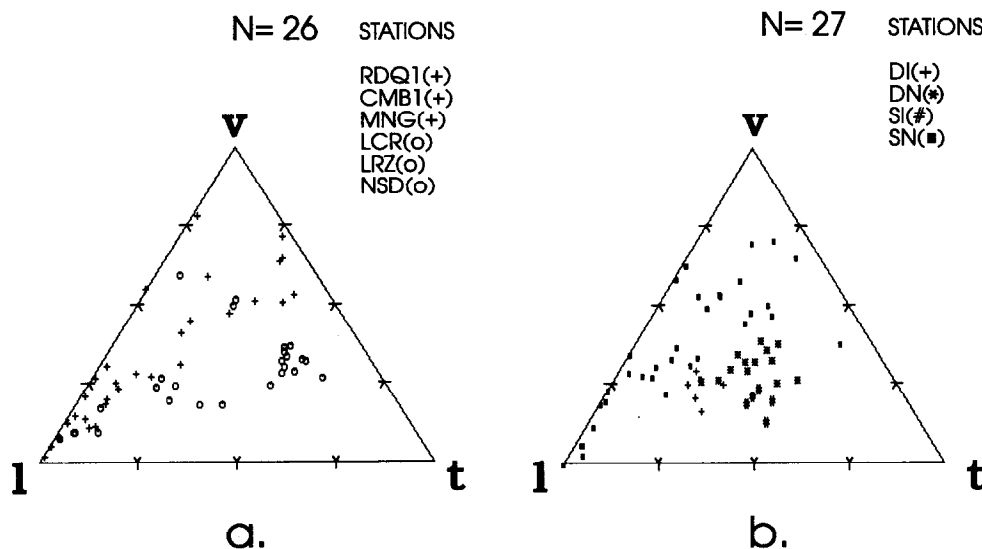


Fig. 3. (a) Faults from different localities. Differences in slip characteristics brought about by the FSC plot. (b) Slip on a fault set with different recorded senses of movement, where: DN, dextral normal; DI, dextral reverse; SN, sinistral normal; and SI, sinistral reverse.

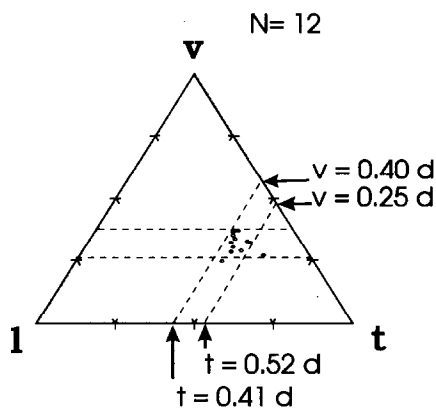


Fig. 4. Data clustering on a FSC diagram for a set of slickensided fault surfaces exposed in a fault scarp. The dashed lines suggest the range of contribution for T and V (derived from t and v) in the net slip.

is known and if a statistical maximum is well defined in the FSC (fault-slip components) diagram. The inverse solution also applies. Figure 4 shows an example of data collected from secondary faults associated with a reverse fault scarp. The topographic displacement of stratigraphic markers across the scarp is 9 m in the example. This information provides the magnitude of the vertical slip (V). The grouping of the fault population in the FSC diagram allows the estimate that: if $0.40d \geq v \geq 0.25d$ (which means $0.40D \geq V \geq 0.25D$) and $V = 9$ m, then the total slip (D) lies between 22.5 and 36 m. Accordingly, if $0.33d \geq t \geq 0.17d$, then the magnitude of T is constrained

to between 9 and 19 m. This trend reflects the contribution of T to the total slip and provides a measure of shortening associated with this set of faults.

The input data for FSC diagrams are the dip and rake data of each fault. For efficient data handling, the assistance of a computer is necessary. The software (ALFA-G) for DOS compatible computers was developed in Turbo Pascal 6.0 (Costa *et al.*, 1992), and is available from the first author.

Acknowledgements—The reviews from D. Ragan and T. Rockwell and their assistance with the final version of the English manuscript is deeply acknowledged. We are also grateful to the other reviewers and to the comments from H. Diederix, C. Gardini and C. Vita-Finzi. This work was supported by the Universidad Nacional de San Luis, Project 348901.

REFERENCES

Angelier, J. (1979) *Néotectonique de l'arc Égéen*. Société Géologique du Nord Publication 3.
 Angelier, J. (1984) Tectonic analysis of fault slip data sets. *Journal of Geophysical Research* **89**, 5835–5848.
 Angelier, J. (1994) Fault slip analysis and paleostress reconstruction. In *Continental Deformation*, ed. P. Hancock, pp. 101–120. Pergamon, Oxford.
 Bott, M. (1959) The mechanisms of oblique slip faulting. *Geological Magazine* **96**, 109–117.
 Costa, C., Gardini, C. and Moran, R. (1992) ALFA-G: Programa para el analisis geométrico de fallas. In *VII Reunión Argentina de Microtectónica Resúmenes*, p. 8. Progeba, Bariloche.